SAND2022-11215C

Quantifying the Effect of CO_2 Gasification on Pulverized Coal Char Oxy-Fuel Combustion

Christopher R. Shaddix[a,*], Ethan S. Hecht[a], Cristina Gonzalo-Tirado[a,b], and Brian S. Haynes[c]

[a] *Combustion Research Facility, Sandia National Laboratories, Livermore, CA 94550, USA*
[b] *Industry and Energy Area, Delegation of Government of Aragón, 50018 Zaragoza, Spain*
[c] *School of Chemical and Biomolecular Engineering, University of Sydney, NSW 2006, Australia*

Abstract

Previous research has provided strong evidence that CO_2 and H_2O gasification reactions can provide non-negligible contributions to the consumption rates of pulverized coal (pc) char during combustion, particularly in oxy-fuel environments. Fully quantifying the contribution of these gasification reactions has proven to be difficult, due to the dearth of knowledge of gasification rates at the elevated particle temperatures associated with typical pc char combustion processes, as well as the complex interaction of oxidation and gasification reactions. Gasification reactions tend to become more important at higher char particle temperatures (because of their high activation energy) and they tend to reduce pc oxidation due to their endothermicity (i.e. cooling effect). The work reported here attempts to quantify the influence of the gasification reaction of CO_2 in a rigorous manner by combining experimental measurements of the particle temperatures and consumption rates of size-classified pc char particles in tailored oxy-fuel environments with simulations from a detailed reacting porous particle model. The results demonstrate that a specific gasification reaction rate relative to the oxidation rate (within an accuracy of approximately +/- 20% of the pre-exponential value), is consistent with the experimentally measured char particle temperatures and burnout rates in oxy-fuel combustion environments. Conversely, the results also show, in agreement with past calculations, that it is extremely difficult to construct a set of kinetics that does not substantially overpredict particle temperature increase in strongly oxygen-enriched N_2 environments. This latter result is believed to result from deficiencies in standard oxidation mechanisms that fail to account for falloff in char oxidation rates at high temperatures.

Keywords: coal; char; oxy-fuel combustion; gasification

---

*Corresponding author.

1. Introduction

The increasing evidence of tangible effects of global climate change has driven government investments and subsidies to promote the adoption of renewable energy technologies. However, many fossil fuel sources offer considerable advantages over renewable energy technologies in terms of land use, energy transport, and energy storage, not to mention readily dispatchable power [1]. Hence, as a strategy to bridge our current fossil-dominated energy systems to a fully renewable energy future in an economically sustainable manner, it is sensible to consider fossil fuel utilization strategies that can result in capture and subsequent use or sequestration of CO_2 generated during energy utilization [2]. Oxy-fuel combustion is one such strategy, and it is a particularly favorable strategy for stationary power generation from coal [3,4] to meet power demands that cannot be met from intermittent renewable power sources. Furthermore, with the potential future generation of large amounts of renewable hydrogen as an energy carrier and as a zero-carbon fuel [5], oxygen may become available as a low-cost 'waste product' from electrolysis of water to produce hydrogen, thereby removing a significant energy efficiency penalty that has historically inhibited the use of oxy-fuel power generation.

As is now well-established in the literature, the replacement of N_2 (in air) with recycled CO_2 and steam in the oxy-fuel combustion process results in impacts throughout the combustion process, due to differences in the radiative, physical, transport, and chemical reaction properties of CO_2 and steam relative to N_2 [3,6-8]. Perhaps the most complex interplay of effects from the replacement of N_2 with CO_2 and H_2O is manifest in the combustion of pulverized char particles, wherein differences in the molar heat capacity, thermal conductivity, mass diffusivity, and both homogeneous and heterogeneous chemical reactivity of the surrounding gases can all influence the combustion process [9]. Of these different factors, the one with the greatest uncertainty is the gasification reactivity of CO_2 (and steam) at the elevated temperatures associated with pulverized coal (pc) char combustion, particularly in oxygen-enriched atmospheres that are often associated with oxy-fuel combustion. The uncertainty in the gasification reaction rates results from (a) a dearth of experimental data on gasification rates at temperatures on the order of 2000 K [10], (b) the high activation energy for these reactions (on the order of 250 kJ/mol [11] for CO_2 gasification), as determined at lower temperatures, which makes extrapolation of rates determined at lower temperatures to higher temperatures fraught, (c) the potential for surface oxide site competition with oxygen and steam reactants, and (d) the potential for suppression of the forward gasification reactions from elevated local concentrations of CO and H_2.

While there have been numerous publications detailing coal and coal char reactivity in oxy-fuel environments at low to intermediate temperatures appropriate for thermogravimetric studies (e.g. see [12]), only a few studies have been reported in the literature that attempt to address the contribution of gasification reactions during oxy-fuel combustion of pc chars at elevated temperatures in a quantitative manner. Geier et al. [13] reported on the fitting of an extended single-film char apparent kinetics reaction model to experimentally measured pc char reaction temperatures measured for two different coals sieved to various size bins burning in an entrained flow reactor operating in O_2-N_2 and O_2-CO_2 environments (with 12-36 vol-% O_2 and 16 vol-% H_2O) around 1700 K. Including the gasification rates (particularly gasification from CO_2) was found to be important to at least roughly predict the measured char combustion temperatures, and the best-fit model yielded a kinetic rate for CO_2 gasification for the two coal chars that was approximately 5×10^{-3} times the value of the kinetic rate for O_2 reaction with the chars, at 2000 K.

Hecht et al. [14] expanded upon the work of Geier et al. by employing a detailed reacting porous particle code, SKIPPY [15], with a combination of intrinsic oxidation and gasification reactions to evaluate the impact of gasification reactions on particle temperature and gas species profiles through the reacting char particles during oxy-fuel combustion. Gasification rates were chosen that yielded approximate agreement with the char particle temperatures measured by Geier et al. [13], but calculations were also performed with gasification rates that were increased by a factor of 5 or neglected altogether, to better illustrate their influence on char combustion. Whereas the gasification reactions were shown to have a strong impact on pc char combustion temperatures, their effect on the net char consumption rate was muted, because of two effects that decreased the rate of oxidation reactions: (1) the lower char combustion temperatures resulting from the strongly endothermic gasification reactions, and (2) the decreased mass diffusivity of oxygen through the particle boundary layer during oxy-fuel combustion (due to elevated CO_2 concentrations). Consequently, it was determined that reductions in the char *oxidation* rate during oxy-fuel combustion partially offset the additional carbon removal from the gasification reactions. Due to the high activation energy of the gasification reactions, their impact was found to be greater when char particle temperatures were higher, and because of the greater penetration of CO_2 and H_2O than O_2 during pc char combustion, the gasification reactions were found to be more significant for larger particles.

Gonzalo-Tirado et al. [16,17] utilized an entrained flow reactor and particle burnout measurements during separate oxidation and gasification experiments to deduce best-fit pc char oxidation and CO_2 gasification single-film apparent kinetics over a gas temperature range of 1300-1700 K, for the full range of coal rank. Similar trends in the partial offset of gasification and oxidation contributions to carbon removal first reported by Hecht et al. [14] were found

in these studies, and gasification reactivity was found to roughly scale with oxidation reactivity across the different rank coal chars. The absolute values of the CO_2 gasification rates determined in these studies are rather high, compared to most others reported in the literature [16,17], and the apparent kinetic rate of CO_2 gasification was found to exceed that for oxidation (for the subbituminous and bituminous coals) for temperatures exceeding 1700 K. Note that the experimental approach taken in the studies by Gonzalo-Tirado et al. inherently presumes there is no competition for active carbon sites during oxy-fuel combustion.

Kim et al. [10] derived a high-temperature single-film apparent kinetic rate for CO_2 gasification of a subbituminous coal, based on nominal fits of combined oxidation and gasification reactions to measured char particle combustion temperatures in an entrained flow reactor operating with 12 and 24 vol-% O_2 in N_2 or in CO_2, at 1700 K [13]. At 2000 K, the apparent kinetic rate for CO_2 gasification derived by Kim et al. is 0.5 times that for O_2 reaction with the char.

Over the past several years, a number of studies have been reported for drop tube measurements of mass loss or flat flame measurements of particle temperatures and mass loss of pulverized coal chars in O_2-N_2 and O_2-CO_2 environments [e.g. 18-19], but these have not yielded true kinetic relationships that can be used to compare the rates of oxidation and gasification reactions. Consequently, as evidenced by the substantial variation reported in the relative rate of CO_2 gasification to oxidation during oxy-fuel combustion of pc char particles, there remains considerable uncertainty in the magnitude of the CO_2 gasification reaction, particularly at the elevated temperatures (> 1700 K) associated with active combustion of pc char. To improve the quantification of this relative rate of CO_2 gasification, we report here a combination of carefully constructed and performed experiments and detailed modeling of reacting porous char particles, wherein relative intrinsic kinetic rates can be evaluated, allowing subsequent extension to apparent rates corresponding to any particular particle size or reaction environment.

2. Experimental Methods

2.1 Entrained flow reactor

Sandia's combustion-driven optical entrained flow reactor was utilized for this study. This reactor has been well characterized and the details of its operation and its utility for char kinetic determinations have been previously reported [20]. A particle-sizing pyrometer was utilized, as described previously, to perform measurements of the char particle size, temperature, and velocity for entrained char particles burning in isolation from one another. To assure good sampling statistics, between 100 and 150 good quality single-particle optical signal traces were collected for each of several selected sampling heights for a given reactor condition. The corresponding particle residence time in the laminar flow furnace was deduced from the measured mean char particle velocities. A N_2-quench, water-cooled isokinetic sampling probe was used to collect char samples at selected reactor heights for subsequent determination of char burnout. The refractory elements Si, Al, and Ti were measured commercially by ICP-OES (inductively coupled plasma optical emission spectrometry) and their concentrations were compared to those in the base char material to calculate the burnout of the organic matter in the char, according to Eq. (1) (written for the case of Ti):

$$\left(m/m_0\right)_{daf} = \left(Y_{Ti}/Y_{Ti,0}\right) * \left[1 - Y_{ash,0} * \left(Y_{Ti}/Y_{Ti,0}\right)\right] / \left(1 - Y_{ash,0}\right) \quad (1)$$

To reduce the effects of data scatter in the determination of burnout according to each refractory metal, the results from the three metals were averaged together.

2.2 Furnace conditions

The choice of furnace operating conditions involved balancing a desire to assure consistent char particle ignition and combustion, while attempting to keep the char combustion temperatures low enough to minimize or eliminate contributions from boundary layer conversion of CO [21], which is favored by high ambient gas temperatures and complicates interpretation of the results. For this reason, a nominal furnace gas temperature of 1300 K was chosen, produced by operating the Hencken burner at an adiabatic flame temperature of approximately 1350 K for N_2 environments and 1400 K for CO_2 environments. Three different oxygen concentrations were utilized: 12, 18, and 24 vol-% O_2, with a total furnace flow of 40 slpm. The balance gas was nominally N_2 or CO_2, although the combustion of fuel gases produced a background steam level of approximately 10 vol-% for the N_2 environments and 13 vol-% for the CO_2 environments (see Table 1). A very low flow of 0.12 slpm unheated N_2 or CO_2 was used to deliver the char particles to the furnace, corresponding to the respective balance gas for the experiments. Furnace gas temperature profiles were measured with a very fine wire (25 μm dia.) type-R thermocouple, corrected for radiant loss [22], which is very minor (~ 15 K) for such a fine thermocouple at this low temperature. As shown in Fig. 1, the gas temperature was quite flat through the reactor and was essentially identical for all flow conditions (the centerline profile shows an initial dip from the effects of the cool feed gas).

2.3 Pulverized char particles

To assure a common char material for the particles reacting in the different reactor environments, high

Table 1
Calculated composition of furnace gases (vol %).

	N_2_12	N_2_18	N_2_24	CO_2_12	CO_2_18	CO_2_24
CO_2	2.5	2.3	2.8	75.0	70.0	62.0
H_2O	10.0	10.5	9.5	13.0	12.0	14.0
N_2	75.5	69.2	63.7			
O_2	12.0	18.0	24.0	12.0	18.0	24.0

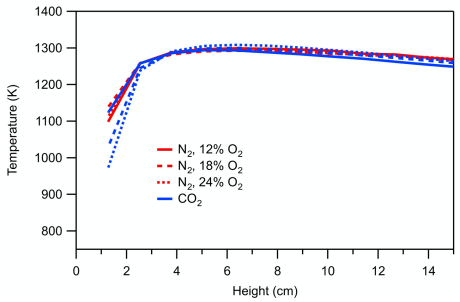

Fig. 1. Centerline gas temperature profiles in the optical entrained flow reactor for the investigated flow conditions.

heating rate char particles were first generated by feeding pre-sieved pulverized low-sulfur subbituminous coal (Black Thunder) particles at a low feed rate into a turbulent entrained flow reactor operating at 1473 K and 1 atm with a preheated N_2 flow with 1.5% O_2 (to prevent tar formation and condensation). The particles were exposed to the high-temperature environment for 250 ms to assure complete devolatilization, before being quenched by cool N_2 flow at the inlet of a water-cooled collection probe. The collected char was size-classified using a mechanical sieve shaker. The 63-75 µm size cut was selected for this study, after re-sieving the particles to remove any residual fines. The use of pre-formed, narrowly-sieved chars provides a well-known char particle diameter, at least for early extents of reaction before the particles shrink, and precludes a reliance on optically measured particle diameters, which typically have an uncertainty of 20% and are limited to char particle sizes greater than 80 µm. Table 2 shows the ultimate and proximate analysis of the raw coal and the prepared char particles. Based on the total ash tracer analysis, the prepared char corresponds to 46% burnout of the raw coal.

Table 2
Composition of coal and prepared char.

wt-%, DAF	coal	char
C	69.0	89.6
H	5.0	0.77
O	25.4	8.0
N	0.97	1.31
S	0.45	0.38
wt-%		
moisture	9.3	3.7
ash	4.8	9.5
volatiles	42.3	12.7
fixed C	43.6	74.1

3. Porous Reacting Particle Modeling

To aide the interpretation of the experimental measurements, we employed the Surface Kinetics in Porous Particle (SKIPPY) code [15,14] developed at the University of Sydney. SKIPPY solves the mass, species, and energy conservation equations inside and outside a porous particle reacting under steady-state conditions in a quiescent environment. From this solution, SKIPPY gives the gas species flows, concentrations and temperature within the pores of the char, at the outer surface of the char, and within the layer of gas surrounding the char. Both heterogeneous (gas-solid) and gas-phase chemical reactions are considered, by employing data and subroutines from the CHEMKIN [23], SURFACE CHEMKIN [24], and Sandia transport [25] packages. A solution is found through the TWOPNT [26] solver and mesh points are automatically added in regions with high gradients.

For the calculations employed here, GRI-MECH 3.0 [27], without nitrogen reactions, was used to describe the gas-phase reaction kinetics. As will be discussed later, several different surface mechanisms were investigated during this study. However, most of the results that will be discussed are based on application of the mechanism shown in Table 3. As in previous uses of SKIPPY [14,15,21,28], the oxidation and gasification reactions are treated as adsorption-limited, with arbitrarily fast desorption reaction rates that guarantee insignificant accumulation of oxygen complexes on the char surface and no competition between O_2 and CO_2 to react with active carbon sites. This neglect of the buildup of oxygen complexes on the char surfaces may contribute to overprediction of the oxidation rate under certain conditions, but does not appear to be a significant factor for the conditions investigated here. Further, by 'calibrating' the CO_2 gasification rate to match experimental trends during oxy-fuel combustion conditions, any competition between O_2 and CO_2 for active carbon sites that is occurring in the experiments is treated semi-empirically. Note that the gasification reactions are written as irreversible. It is possible that some inhibition of the forward reaction occurs under some of the conditions investigated here (esp. 24% O_2 in CO_2), but the ability of this mechanism to match the experimental measurements suggests the effect is not too large.

Table 3
Heterogeneous oxidation and gasification mechanism.

Reaction	A (units of mol,cm,s)	E (kJ/mol)
$C_b + C_s + O_2 \rightarrow CO + C(O)_s$	3.30×10^{15}	167.4
$C(O)_s + C_b \rightarrow CO + C_s$	1.00×10^{8}	0
$C_s + O_2 \rightarrow C(O_2)_s$	9.50×10^{13}	142.3
$C(O_2)_s + C_b \rightarrow CO_2 + C_s$	1.00×10^{8}	0
$C_s + CO_2 \rightarrow CO + C(O)_s$	2.16×10^{15}	251.0
$C_s + H_2O \rightarrow H_2 + C(O)_s$	2.61×10^{14}	222.0

4. Results and Discussion

4.1 Char particle combustion temperatures

Figure 2 shows the char particle temperatures measured in the N_2 and CO_2 environments, as a function of char particle residence time, together with some of the calculated char particle temperatures from the SKIPPY simulations. The experimental data are shown as box plots [29] to indicate the statistical distribution of measured char temperatures at each axial position for a given flow condition. The size of the 25-75 percentile box edges (i.e. the 'H-spread') of the measurements indicates the combined effects of the 2-color pyrometry precision and the variation in the size and composition (reactivity) of the char feed particles. For the measurements performed during intermediate stages of burnout the H-spread is relatively small (order of 25 K in N_2 and 50 K in CO_2). The H-spread is enlarged at low and high measurement heights, where incompletely ignited particles (at low heights) or partly extinguished particles (at high heights) are likely present within the measured particle population, contributing to enhanced variance in the distribution of single particle temperatures.

The calculations are focused on predicting the experimental trends during intermediate extents of burnout, to minimize uncertainties due to the effects of transient char ignition or extensive burnout. Predicting the full particle temperature temporal profiles would require introducing a statistical particle reactivity distribution (with unknown parameters) as well as a burnout model (again, with unknown parameters), neither of which would add any rigor to an analysis of the base oxidation and gasification rates, which is the focus here.

Figure 2 shows the expected strong dependence of char combustion temperature on the oxygen concentration of the furnace gas, for both N_2 and CO_2 environments. For a given bulk O_2 concentration, the char combustion temperature in CO_2 is consistently lower than that in N_2, by 100–150 K, reflecting the combined effects of an approximately 17% lower diffusivity of oxygen through CO_2 in the particle boundary layer and the endothermic reaction of CO_2 with the char.

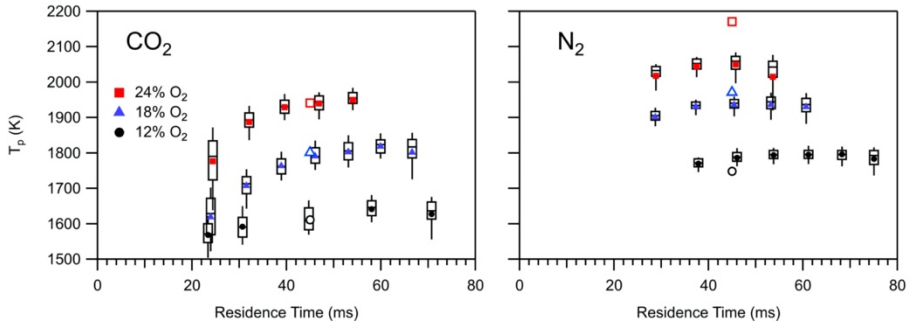

Fig. 2. Measured and modeled char particle temperatures as a function of residence time in the entrained flow reactor for CO_2 and N_2 environments. The mean particle temperatures are shown as solid symbols, whereas the box and whiskers surrounding the data points indicate the 25-75 percentile limits (box edges) and the 10-90 percentile limits (whiskers) of the measured distribution of single-particle statistics at each sampling location. The open symbols at a residence time of 45 ms indicate char particle temperatures calculated by SKIPPY for the corresponding gas conditions using the mechanism shown in Table 3 (a height of 5 cm in the reactor corresponds to a residence time of 38 ms).

4.2 Char burnout

Figure 3 shows the measured burnout, as determined from char collection and analysis via the refractory ash tracer technique. Even after averaging the three measured refractory metals, there is some noise evident in the profiles. Due to the difficulty in collecting sufficient sample mass for analysis when feeding char particles at a low enough feed rate to assure isolated particle combustion, only single samples were collected at each height. Table 4 shows the values of the line fits that were determined for the different experimental conditions, as well the burning rates calculated from SKIPPY, using the mechanism shown in Table 3. A fully quantitative comparison between the SKIPPY burning rates and the experimental rates is not possible, because of uncertainty over the actual char particle densities, particularly as the char burns out. However, it should be noted that a 70 μm diameter char particle with 10% ash content (as is modeled in the SKIPPY simulations) and a density of 0.7 g/cm^3 has a carbon content of 9.3 x 10^{-9} moles, such that a simulated conversion rate of 10^{-8} mol/s approximately corresponds to an experimental burnout rate of 1/s, which is why the computational rates are shown in units of 10^{-8} mol/s in Table 3. The experimental burning rates are quite similar for the chars burning in the N_2 and CO_2 environments *for a given oxygen concentration*, and probably cannot be distinguished from one another within the measurement uncertainty. The calculated burnout trends are similar to the

experimental trends, except that the simulated burnout in N_2 environments is consistently higher than that in CO_2 environments, which is due, at least in part, to overpredictions of char particle temperatures in N_2 environments, as will be discussed below.

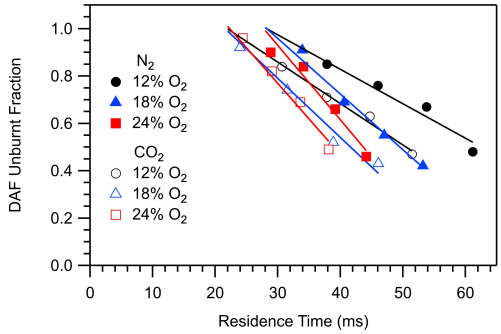

Fig. 3. Measured dry, ash-free burnout of the char particles as a function of residence time in the entrained flow reactor for N_2 and CO_2 environments. Line fits to the data are shown.

Table 4
Char burning rates.

bath gas	O_2 vol-%	measured burning rate (1/s)	calculated burning rate (10^{-8} mol/s)
N_2	12.0	14.5	17.3
	18.0	23.4	29.9
	24.0	31.4	41.1
CO_2	12.0	17.5	13.2
	18.0	24.9	23.6
	24.0	30.1	33.2

4.3 SKIPPY studies of surface kinetics

SKIPPY simulations were conducted in a systematic manner to deduce the best-fit CO_2 gasification rate, relative to the oxidation rate, for the experimental measurements of char particle combustion temperatures in the N_2 and CO_2 environments. The presumed surface area, which combines with the C active site density (assumed to be 1.7 x 10^{-9} mol/cm^2 [15]) to yield the mass-specific site density, was varied, together with the presumed gasification rate, until nearly perfect agreement was obtained with char combustion temperatures in the CO_2 environment, which naturally is more sensitive to the CO_2 gasification reaction. This agreement was obtained using a presumed surface area of 43 m^2/g and the gasification rates shown in Table 3. Note that during high temperature combustion and gasification there is strong evidence that little of the micropore surface area is accessed, such that use of surface areas characteristic of mesopores for these calculations is appropriate, as has been previously discussed [14]. The best-fit presumed surface area and gasification rate could be derived by independently varying these two parameters because the char combustion temperature in the 12% O_2 environment is very sensitive to the presumed surface area, but is fairly insensitive to the gasification rate, whereas in the 24% O_2 environment the opposite is true. This behavior presumably results from the high temperature sensitivity of the CO_2 gasification reaction (due to its high activation energy).

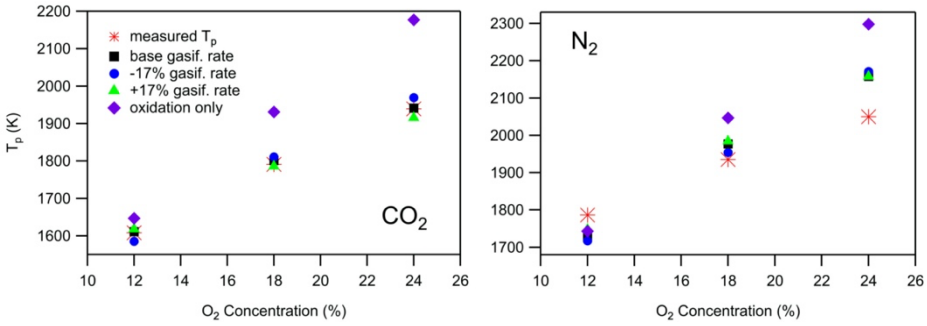

Fig. 4. Measured and modeled char particle temperatures for the CO_2 and N_2 environments, wherein different assumptions were made regarding the relative intensity of the CO_2 and steam gasification reactions. Note that the same scale is used for the y-axis of these two plots, but they cover different ranges.

Figure 4 shows results for measured and various simulated char particle temperatures in both the CO_2 and N_2 environments. As noted before, the best way to compare kinetic model predictions is to focus on the quasi-steady burning associated with moderate amounts of char burnout, so the comparisons are made at a residence time of 45 ms. In the CO_2 environments, use of gasification rates that were 17% higher and lower gave somewhat worse results than for the 'best-fit' base gasification kinetic rates. For example, for 24% O_2 in CO_2, the use of the higher gasification rate underpredicted the char temperature by 25 K, whereas the lower gasification rate led to a 30 K overprediction. Attempting to match the experimental data when using an oxidation-only mechanism dramatically failed, particularly in the CO_2 environment for 18% and 24% O_2. The oxidation-only mechanism also gave poor predictions in the N_2

environment for 18% and especially 24% O_2, due to the gasification reactions attributed to the moisture and (low) CO_2 content in the furnace gases, combined with CO_2 locally generated in the particle boundary layer from oxidation of CO.

As is apparent from Fig. 4, whereas the particle temperatures measured in the CO_2 environments with 12-24 vol-% O_2 can be well-described by the SKIPPY model when using the oxidation and gasification rates shown in Table 3, the same is not true in N_2 environments, most notably in the case of 24 vol-% O_2, when the char combustion temperature exceeds 2000 K. This trend of combustion models overpredicting char particle combustion temperatures for elevated ambient oxygen concentrations has been reported several times before [13,14,20,28]. To further probe this, SKIPPY simulations were performed in which the presumed activation energy of both oxidation reactions shown in Table 3 was decreased, from 167.4 kJ/mol (40 kcal/mol) to 125.5 kJ/mol (30 kcal/mol) for the primary oxidation reaction, leading to CO formation. The overall oxidation rate was maintained constant at 1900 K through adjustment of the pre-exponentials. With this adjustment, the predicted char particle temperature for 18% O_2 in N_2 remained the same, while the temperature in 12% O_2 in N_2 increased by approximately 30 K and the temperature in 24% O_2 in N_2 decreased by approximately 20 K. While these are improvements, in comparison to the experimental data, the char temperature was still well over-predicted for 24% O_2 in N_2.

As mentioned in Section 3, char particle oxidation calculations have traditionally neglected competition for C active sites. Also, measurements of the intrinsic reaction order for oxidation of carbon chars tend to cluster around 0.7 [30], which is not reflected in the simplified oxidation mechanism shown in Table 3. To rectify these deficiencies, we implemented the five-step oxidation mechanism developed by Geier et al. [31] into SKIPPY. This mechanism explicitly accounts for the oxygen partial pressure dependence of the overall oxidation rate and accounts for competition between the different steps for active sites. With this more sophisticated oxidation mechanism, we obtained nearly identical char particle temperature predictions in N_2 environments, and worse predictions in CO_2 environments.

Recent molecular beam oxidation experiments with vitreous carbon have revealed that at high temperatures, the oxidation rate becomes attenuated due to prompt dissociation of surface oxides from the carbon surface (i.e. O atom desorption), with an activation energy of approximately 370 kJ/mol [32-33], which corresponds to the strength of a typical C-O bond [34]. This new mechanistic finding is consistent with some previous studies of carbon oxidation by O_2 that found retarded high-temperature carbon oxidation (e.g. [35-36]), which until now has not been explained. These results suggest that existing char oxidation mechanisms are missing a key reaction step that plays an increasingly important role at high char temperatures – a step that should provide better agreement of model predictions with measurements for char oxidation at elevated oxygen concentrations, particularly in N_2 environments where the particle temperatures are higher. Also, it should be noted that thermal annealing effects on char reactivity [37] are not currently included in our char reaction model and could play a role in the overprediction of char particle temperatures in oxygen-enriched environments.

4.4 SKIPPY simulations of gas profiles

Figure 5 shows the computed gas concentration and temperature profiles through the char particle and in the vicinity of the particle for the investigated CO_2 environments, using the best-fit gasification kinetic rates. There are several things to note: (a) CO, a byproduct of both oxidation and CO_2 gasification reactions, builds up to increasingly large values as the O_2 content increases in the bath gas, until it reaches over 70 mol-% in the center of the char particle when burning in 24% O_2, (b) the CO_2 concentration in the particle falls rapidly as the bulk O_2 content increases, as a result of both an increase in CO production in the particle and an increase in consumption of CO_2 via the gasification reaction (which is highly temperature dependent), (c) O_2 does not penetrate the char very far, particularly at the higher char temperatures associated with combustion at elevated bulk O_2 levels (the calculated effectiveness factor for O_2 decreases from 18.5% in the 12% O_2 condition to 8.1% for the 24% O_2 condition), (d) the 14% steam in the bulk gas results in a small amount of H_2 production in the char at the 24% O_2 condition, from the steam gasification reaction, and (e) the minor increase in the concentration of CO_2 just outside of the particle for elevated O_2 conditions indicates some boundary layer conversion of CO is occurring. The reaction-specific carbon consumption data from the simulations shows that the CO_2 gasification reaction accounts for 5.4% of the carbon removal for the 12% O_2 condition, 13.6% for the 18% O_2 condition, and 19.5% for the 24% O_2 condition. These results highlight the complexity of the role of the gasification reactions during oxy-fuel combustion of pc chars.

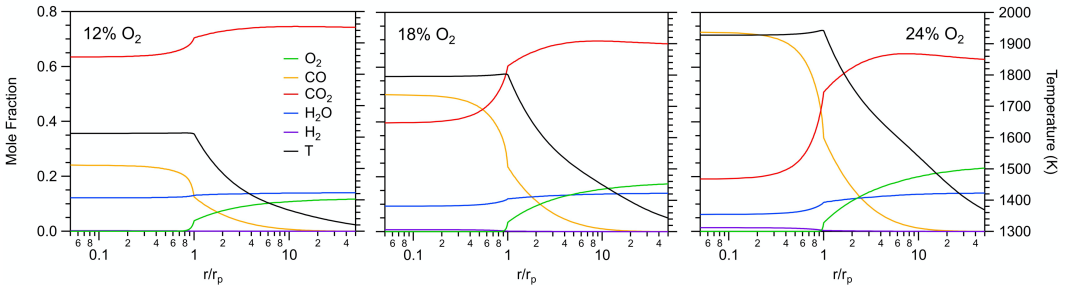

Fig. 5. Computed temperature and gas species profiles for 70 µm char particles reacting in O_2/CO_2 mixtures at 1300 K, using the gasification kinetics shown in Table 3. The radial position from the char particle center has been normalized by the particle radius and is displayed on a logarithmic scale.

4.5 Rate comparisons with literature

The magnitude of the best-fit oxy-fuel gasification kinetic rates determined in this study appear to be lower than many of those that have been recently reported, but direct comparisons of the intrinsic kinetics determined here with apparent reaction rates determined under different reaction conditions are difficult. On the other hand, the rates determined here are only 40% lower than the intrinsic kinetic rates used by Hecht et al. [14] to roughly match experimentally measured oxy-fuel char combustion temperatures using SKIPPY and appear to be in good agreement with the apparent kinetics rates determined by Geier et al. [13]. The advantage of focusing on the determination of intrinsic kinetic rates, as done in this study, is that these rates can be readily converted to apparent rates, as used in large-scale computational fluid dynamic simulations of coal combustion, for a given particle size, temperature, and surrounding gas environment.

5. Conclusions

A narrow size cut (approx. 70 µm in diameter) of a high heating rate subbituminous coal char was combusted in an entrained flow reactor operating at 1300 K with O_2-N_2 and O_2-CO_2 mixtures varying from 12-24 vol-% O_2. Measured char particle temperatures are 100-150 K higher in the N_2 environments, but the measured burnout rates in the two environments are similar for a given bulk oxygen concentration. Detailed particle simulations with the SKIPPY code match the experimental char combustion temperatures in the CO_2 environments when using a CO_2 gasification rate that is somewhat lower than one previously utilized in an earlier, less rigorous SKIPPY analysis. The SKIPPY simulations also show reasonable agreement with the measured burnout rates in the CO_2 environments. Comparisons of the simulations and the experimental measurements are less satisfying in the N_2 environments, due to an overprediction of char reaction temperatures for elevated bulk oxygen levels. Recent results in the literature suggest that this overprediction of char particle temperatures in oxygen-enriched N_2 environments may result from the neglect of a key reaction step in char oxidation mechanisms, or from thermal annealing effects. Even with the somewhat lower CO_2 gasification rate determined in this study, its influence on the char combustion process in O_2-CO_2 environments is significant, particularly for elevated char combustion temperatures.

Acknowledgements

Support for this research was provided by the U.S. Department of Energy through the National Energy Technology Laboratory's Cross-Cutting Research Program. The assistance of Dr. Jinhan Yun (KIMM, South Korea) in collecting char samples for this work is greatly appreciated. Sandia National Laboratories is a multimission laboratory managed and operated by National Technology and Engineering Solutions of Sandia, LLC., a wholly owned subsidiary of Honeywell International, Inc., for the U.S. Department of Energy's National Nuclear Security Administration under contract DE-NA-0003525. The views expressed in the article do not necessarily represent the views of the U.S. Department of Energy or the United States Government.

References

[1] P. Das, J. Mathur, R. Bhakar, A. Kanudia, Implications of short-term renewable energy resource intermittency in long-term power system planning, *Energy Strateg. Rev.* 22 (2018) 1-15.

[2] N.A. Sepulveda, J.D. Jenkins, F.J. de Sisternes, R.K. Lester, The role of firm low-carbon electricity resources in deep decarbonization of power generation, *Joule* 2 (2018) 2403-2420.

[3] B.J.P. Buhre, L.K. Elliott, C.D. Sheng, R.P. Gupta, T.F. Wall, Oxy-fuel combustion technology for coal-fired power generation, *Prog. Energ. Combust.* 31 (2005) 283-307.

[4] S. Chen, Y. Zheng, M. Wu, J. Hu, W. Xiang, Thermodynamic analysis of oxy-fuel combustion integrated with the sCO_2 Brayton cycle for combined heat

and power production, *Energ. Convers. Manage.* 232 (2021) 113869.
[5] T. Capurso, M. Stefanizzi, M. Torresi, S.M. Camporeale, Perspective of the role of hydrogen in 21st century energy transition, *Energ. Convers. Manage.* 251 (2022) 114898.
[6] M.B. Toftegaard, J. Brix, P.A. Jensen, P. Glarborg, A.D. Jensen, Oxy-fuel combustion of solid fuels, *Prog. Energ. Combust.* 36 (2010) 581-625.
[7] L. Chen, S.Z. Yong, A.F. Ghoniem, Oxy-fuel combustion of pulverized coal: characterization, fundamentals, stabilization and CFD modeling, *Prog. Energ. Combust.* 38 (2012) 156-214.
[8] C. Yin, J. Yan, Oxy-fuel combustion of pulverized fuels: combustion fundamentals and modeling, *Appl. Energ.* 162 (2016) 742-762.
[9] C. Shaddix, A. Molina, in L. Zheng (Ed.), Oxy-fuel combustion for power generation and carbon dioxide (CO_2) capture, Woodhead Publishing, Cambridge UK, 2011, pp. 101-124.
[10] D. Kim, S. Choi, C.R. Shaddix, M. Geier, Effect of CO_2 gasification reaction on char particle combustion in oxy-fuel conditions, *Fuel* 120 (2014) 130-140.
[11] N.M. Laurendeau, Heterogeneous kinetics of coal char gasification and combustion, *Prog. Energ. Combust.* 4 (1978) 221-270.
[12] G. Varhegyi, P. Szabo, E. Jakab, F. Till, J.R. Richard, Mathematical modeling of char reactivity in Ar-O_2 and CO_2-O_2 mixtures, *Energ Fuels* 10 (1996) 1208-1214.
[13] M. Geier, C.R. Shaddix, K.A. Davis, H.-S. Shim, On the use of single-film models to describe the oxy-fuel combustion of pulverized coal char, *Appl Energ* 93 (2012) 675-679.
[14] E. Hecht, C.R. Shaddix, M. Geier, A. Molina, B.S. Haynes, Effect of CO_2 and steam gasification reactions on the oxy-combustion of pulverized coal char, *Combust. Flame* 159 (2012) 3437–3447.
[15] P.J. Ashman, B.S. Haynes, Improved techniques for the prediction of NOx formation from char nitrogen, Project No. C4065; Australian Coal Association. CSIRO Energy Technology: North Ryde NSW, Australia, 1999.
[16] C. Gonzalo-Tirado, S. Jimenéz, J. Ballester, Gasification of a pulverized sub-bituminous coal in CO_2 at atmospheric pressure in an entrained flow reactor *Combust. Flame* 159 (2012) 385-395.
[17] C. Gonzalo-Tirado, S. Jimenéz, J. Ballester, Kinetics of CO_2 gasification for coals of different rank under oxy-combustion conditions, *Combust. Flame* 160 (2013) 411-416.
[18] Y. Niu, S. Liu, B. Yan, S. Wang, X. Zhang, S. Hui, Effects of CO_2 gasification reaction on the combustion of pulverized coal char, *Fuel* 233 (2018) 77-83.
[19] O. Senneca, N. Vorobiev, A. Wütscher, F. Cerciello, S. Heuer, C. Wedler, R. Span, M. Schiemann, M. Muhler, V. Scherer, Assessment of combustion rates of coal chars for oxy-combustion applications, *Fuel* 238 (2019) 173-185.
[20] J.J. Murphy, C.R. Shaddix, Combustion kinetics of coal chars in oxygen-enriched environments, *Combust. Flame* 144 (2006) 710–729.
[21] E. Hecht, C.R. Shaddix, A. Molina, B.S. Haynes, Effect of CO_2 gasification reaction on oxy-combustion of pulverized coal char, *Proc. Combust. Inst.* 33 (2011) 1699–1706.
[22] C.R. Shaddix, Proceedings of the 33rd National Heat Transfer Conference, HTD99-282, ASME, New York, NY, 1999.
[23] R.J. Kee, F.M. Rupley, J.A. Miller, CHEMKIN II: A Fortran Chemical Kinetics Package for the Analysis of Gas-Phase Chemical Kinetics. SAND 89-8009, Sandia National Laboratories, CA, 1989.
[24] M.E. Coltrin, R.J. Kee, F.M. Rupley, Surface Chemkin (Version 3.7): A Fortran Package for Analyzing Heterogeneous Chemical Kinetics at a Solid-Surface-Gas-Phase Interface. SAND90-8003, Sandia National Laboratories, CA, 1990.
[25] R.J. Kee, G. Dixon-Lewis, J. Warnatz, M.E. Coltrim, J.A. Miller, A Fortran Computer Code Package for the Evaluation of Gas-Phase, Multicomponent Transport Properties. SAND 86-8246, Sandia National Laboratories, CA, 1986.
[26] J.F. Grcar, The twopnt program for boundary value problems, SAND-91-8230; Sandia National Labs: Livermore, CA, (USA), 1992.
[27] G.P. Smith, S.D. Golden, M. Frenklach, N.W. Moriarty, B. Eitener, M. Goldenberg, C.T. Bowman, R.K. Hanson, S. Song, W.C. Gardiner, V.V. Lissianski, Z. Qin, GRI-MECH 3.0, 2001. http://www.me.berkeley.edu/gri_mech
[28] C.R. Shaddix, E.S. Hecht, C. Gonzalo-Tirado, B.S. Haynes, The effect of bulk gas diffusivity on apparent pulverized coal char combustion kinetics, *Proc. Combust. Inst.* 37 (2019) 3071-3079.
[29] J.W. Tukey. Exploratory Data Analysis. Addison–Wesley Pub. Co., Reading, MA, 1977.
[30] E.M. Suuberg, M. Wójtowicz, J.M. Calo, Reaction order for low temperature oxidation of carbons, *Proc. Combust. Inst.* 22 (1989) 79-87.
[31] M. Geier, C.R. Shaddix, F. Holzleithner, A mechanistic char oxidation model consistent with observed CO_2/CO production ratios, *Proc. Combust. Inst.* 34 (2013) 2411-2418.
[32] S. Poovathingal, T.E. Schwartzentruber, V.J. Murray, T.K. Minton, G.V. Candler, Finite-rate oxidation model for carbon surfaces from molecular beam experiments, *AIAA J.* 55 (2017) 1644-1658.
[33] K. Swaminathan-Gopalan, A. Borner, V.J. Murray, S. Poovathinga, T.K. Minton, N.N. Mansour, K.A. Stephani, Development and validation of a finite-rate model for carbon oxidation by atomic oxygen, *Carbon* 137 (2018) 313-332.
[34] T.L. Cottrell, The Strengths of Chemical Bonds, 2nd ed., Butterworths, London, 1958, pp. A-21–A-34.
[35] J. Nagle, R.F. Strickland-Constable, Oxidation of carbon between 1000-2000 C, Proceedings of the Fifth Carbon Conference, Vol. 1, Pergamon Press, New York, 1962.
[36] D.E. Rosner, H.D. Allendorf, Comparative studies of the attack of pyrolytic and isotropic graphite by atomic and molecular oxygen at high temperatures, *AIAA J.* 6 (1968) 650–654.
[37] T. Holland, T.H. Fletcher, O. Senneca, Review of carbonaceous annealing effects on O_2 and CO_2 coal reactivity, *Energy Fuels* 33 (2019) 10415-10434.